Damghan University Press

Journal of Nano Simulation
journal homepage: jons.du.ac.ir

Volume 1, Issue 1, Winter 2025, 9-15
DOI: 10.22128/jons.2025.951.1000

# Intramolecular hydrogen bond and tautomeric stability of 5-Bromo-salicylideneiminpo-ethylimino-pentan-2-one

Vahidreza Darugar[1]*, Mahmood Akbari[2], Ali Reza Berenji[3]

[1] *Department of Chemistry, Faculty of Science, Ferdowsi University of Mashhad, Iran*
[2] *UNESCO-UNISA-ITL/NRF Africa Chair in Nanoscience and Nanotechnology, College of Graduate Studies, University of South Africa (UNISA), Muckleneuk Ridge, P.O. Box 392, Pretoria, South Africa*
[3] *Department of Chemistry, Faculty of Science, University of Gonabad, Gonabad 96919, Iran*

## H I G H L I G H T S

- L3, L4 tautomers are more stable than the L1, L2 tautomers.
- With increasing polarity of the solvents, L3 form finds more stability.
- The following trend in hydrogen bond strength is concluded: BrSEIPO > SEIPO > APO.

## G R A P H I C A L A B S T R A C T

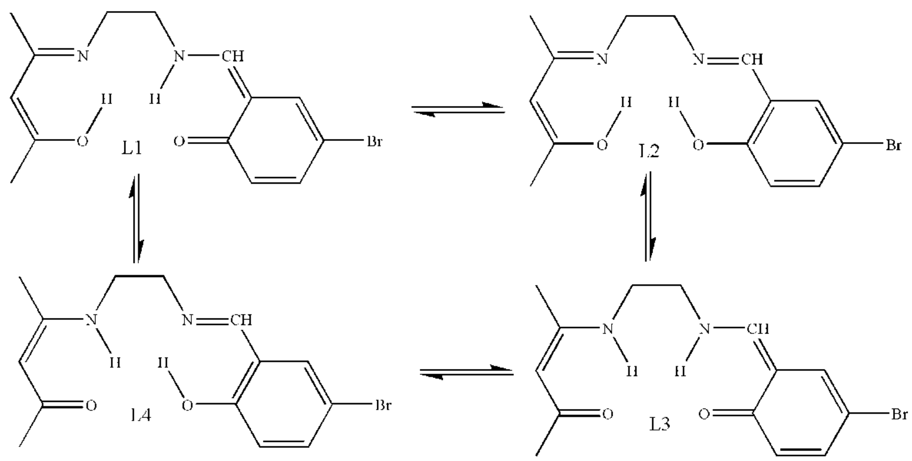


## ARTICLE INFO

*Article history:*
Received: 2025-03-11
Received in revised form: 2025-04-17
Accepted: 2025-05-24

Available online: 2025-06-23

*Keywords:*
Tetradentate Schiff bases,
Tautomerism,
Density functional theory

## ABSTRACT

The tautomerism and intramolecular hydrogen bond of 5-Bromo-salicylideneimino-ethylimino-pentan-2-one (BrSEIPO) was studied by theoretical method. The tautomeric mole fraction calculations show that the L4 and L3 forms are the more stable form of SEIPO with 99.29% and 0.71% values in gas phase and for L4 form more than 67.91% in solution phase. It can be seen that with increasing the polarity of the solvent the molar fractions of two more stable forms are changed. The molar fraction of L4 and L3 forms decreases and increases, respectively Besides, the mole fraction of L3 tautomer becomes in the range from ca. 0.87% to 33.69%, while the polarity of solvent increases. By comparing the value of the geometrical results (RO…N, RN–H, O…H, θOHN), AIM results ($\rho_{BCP}$, $\nabla^2\rho_{BCP}$, $H_{BCP}$, H-bond energy), and spectroscopic result (νNH, γNH, δOH) it can be see that the intramolecular hydrogen bonding (IHB) of BrSEIPO is stronger than that in salicylideneimino-ethylimino-pentan-2-one (SEIPO) and 4-amino-3-penten-2-one (APO).

*Email: vahidrezadarugar@gmail.com

## 1. Introduction

The tetradentate Schiff bases with an $N_2O_2$ donor group have received special attention due to being able to coordinate to different metal ions[1], formation metallo-organic complexes [2,3] and coordination compounds with diamine [4], salen-type [5,6], pyridine [7,8]. Asymmetrical Schiff base ligands are one of the most important compounds and received much attention due to the bounding of central metal ions with asymmetrical ligands in natural systems [9] and also optoelectronic, electrochemical and magnetic properties [10].

α,β-unsaturated-β-ketoenamines, are capable to exist in three different tautomers at equilibrium, i.e., ketoimine, aminoketone, and iminoenol forms. The aminoketone and iminoenol forms of β-Enaminones are more stable than ketoimine form. Therefore, we investigate the behavior of tautomerism in these two more stable forms. Schiff bases with the $N_2O_2$ group coexistence of different isomeric forms, the aminoketone and iminoenol tautomers are engaged in a six-member ring by intramolecular hydrogen bonded system, with the N-H...O and O-H...N systems, respectively [11]. The calculated electronic energies of aminoketone forms are usually less than those of imino enol forms. This is in agreement with the reported studies, which is shown the aminoketone forms as a major form in β-Enaminones [12-14].

Hydrogen bonds are a key aspect of molecular structure and are one of the most important interactions in many chemical and biochemical processes. The N-H...O system is more important than the O-H...O bond because of its importance in protein folding, DNA pairing and so on [15-17].

Some of the effective factors such as temperature, the polarity of the solvent, and type of α and β substitutions can change the mentioned tautomerization equilibrium. These effective factors were studied by theoretical and experimental methods such as quantum-mechanical calculation, IR, Raman, microwave, UV, and NMR spectroscopies, X-ray, electron, and neutron diffraction measurements [12-14, 18-22].

The aim of this research is the study of tautomerism stability (see Figure 1) and comparison its intramolecular hydrogen bond strength with familiar molecules by theoretical and experimental methods.

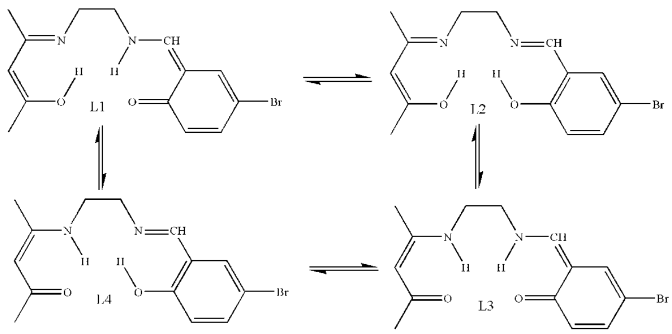


**Figure 1** Possible tautomeric forms of 5-Bromo-salicylideneimino-ethylimino-pentan-2-one.

## 2. Computational details

All calculations of the four tautomers of the title compound were calculated using B3LYP/6-311++G(d,p) method using GAUSSIAN 03 program package [23]. The electronic properties are computed with the time-dependent DFT (TD-DFT) method with polarizable continuum models (PCM) [24]. AIM 2000 software [25] was applied to obtain an electron density at the hydrogen bond critical points. The natural atomic charges and charge transfer energies ($E^2$) are calculated via the NBO analysis.

## 3. Results and Discussion

### 3.1 Conformational studies and optimized geometry

Structural optimization calculations for four tautomers in the gas and solution phases are done and relative energies presented in Table 1. The L4 form has the most stability. The tautomeric mole fraction (according to their calculated ΔG energies [26]) show that the L4 and L3 forms are the more stable forms with 99.29% and 0.71% values in the gas phase. The selected solvents for comparison of mole fractions are $CCl_4$ (ε=2.2), $C_2H_5OH$ (ε=24.5), and $CH_3CN$ (ε=37.5). Based on the results of Table 1, it can be seen that with increasing the polarity of the solvent the molar fractions of two more stable forms are changed. The molar fraction of L4 and L3 forms decreases and increases, respectively. The L3 form has more polarity than L4 form; therefore, with increasing solvent polarity L3 form becomes more stable and the molar fraction increases from 0.87 to 33.69.

As mentioned in conformational studies, the L3 form has a greater polarity than L4 form and with increased the polarity of the solvent the molar fraction of L3 form increases (see table 1). Table 1 show that increasing polarity of the solvent is not enough for the appearance of L3 form, in acetonitrile with

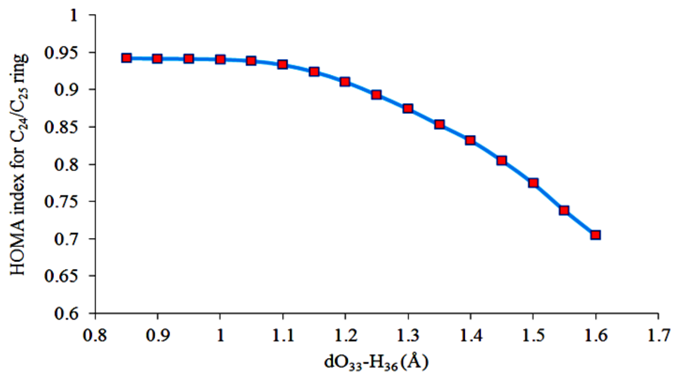


**Figure 2.** The changes in HOMA index of $C_{24}/C_{25}$ ring during the proton transfer process.

**Table 1:** The selected molecular features for the L1, L2, L3 and L4 tautomers forms at DFT-B3LYP/6-311++G(d,p) level of theory.

| | Gas | | | | $CCl_4$ | | | | EtOH | | | | $CH_3CN$ | | | |
|---|---|---|---|---|---|---|---|---|---|---|---|---|---|---|---|---|
| | L1 | L2 | L3 | L4 | L1 | L2 | L3 | L4 | L1 | L2 | L3 | L4 | L1 | L2 | L3 | L4 |
| μ(Debye) | 4.92 | 2.60 | 4.05 | 2.09 | 7.54 | 4.95 | 7.54 | 2.53 | 9.73 | 5.99 | 5.03 | 3.20 | 9.83 | 6.03 | 6.43 | 3.23 |
| $\Delta E_0$(kcal/mol) | 9.530 | 6.32 | 3.20 | 0.00 | 8.43 | 7.07 | 8.43 | 0.00 | 7.42 | 8.02 | 1.81 | 0.00 | 7.34 | 8.04 | 0.30 | 0.00 |
| ΔG(kcal/mol) | 9.51 | 6.59 | 2.92 | 0.00 | 8.38 | 7.23 | 2.81 | 0.00 | 7.71 | 8.46 | 1.60 | 0.00 | 7.40 | 8.43 | 0.44 | 0.00 |
| Mole fractions (%) | 0.00 | 0.00 | 0.71 | 99.29 | 0.00 | 0.00 | 0.87 | 93.76 | 0.00 | 0.00 | 32.09 | 66.31 | 0.00 | 0.00 | 33.69 | 67.91 |

**Table 2:** Optimized geometrical parameters of BrSEIPO at B3LYP/6-311++G(d,p) level.

| Parameters | B3LYP | | | | X-ray | X-ray |
|---|---|---|---|---|---|---|
| Bond lengths (Å) | L1 | L2 | L3 | L4 | | |
| $C_{1}$-$C_{2}$ | 1.369 | 1.368 | 1.437 | 1.435 | 1.419[a] | 1.413[b] |
| $C_{1}$-$C_{3}$ | 1.446 | 1.448 | 1.385 | 1.386 | 1.381[a] | 1.390[b] |
| $C_{2}$-$O_{13}$ | 1.328 | 1.328 | 1.248 | 1.248 | 1.232[a] | 1.241[b] |
| $H_{34}$-$N_{14}$ | 1.611 | 1.605 | 1.028 | 1.027 | 0.857[a] | 0.860[b] |
| $O_{13}$…$H_{34}$ | 1.021 | 1.023 | 1.786 | 1.798 | 1.981[a] | 2.021[b] |
| $N_{14}$-$C_{3}$ | 1.303 | 1.300 | 1.352 | 1.348 | 1.317[a] | 1.328[b] |
| $N_{14}$-$O_{13}$ | 2.546 | 2.543 | 2.646 | 2.654 | 2.692[a] | 2.702[b] |
| $C_{22}$-$C_{24}$ | 1.303 | 1.300 | 1.352 | 1.348 | 1.454[c] | |
| $C_{24}$-$C_{26}$ | 1.447 | 1.449 | 1.446 | 1.449 | 1.394[c] | |
| $C_{22}$-$N_{19}$ | 1.403 | 1.456 | 1.401 | 1.454 | 1.269[c] | 1.278[d] |
| $N_{19}$…$H_{36}$ | 1.463 | 1.419 | 1.463 | 1.419 | 1.858[c] | 1.780[d] |
| $H_{36}$-$O_{33}$ | 1.714 | 0.998 | 1.702 | 0.996 | 0.829[c] | 0.940[d] |
| $N_{19}$-$O_{33}$ | 2.590 | 2.619 | 2.583 | 1.726 | 2.610[c] | 2.613[d] |
| $C_{26}$-$O_{33}$ | 1.453 | 1.452 | 1.322 | 1.450 | 1.337[c] | 1.351[d] |
| Bond angles (°) | | | | | | |
| A(1,2,13) | 122.0 | 122.0 | 123.1 | 123.2 | 123.9[a] | 123.6[b] |
| A(1,3,14) | 118.4 | 118.5 | 120.4 | 120.7 | 121.4[a] | 121.7[b] |
| A(13,34,14) | 149.8 | 150.0 | 138.6 | 138.5 | 136.4[a] | 135.5[b] |
| A(24,22,19) | 123.2 | 122.4 | 123.0 | 122.5 | 122.8[c] | 121.5[d] |
| A(24,26,33) | 122.1 | 121.7 | 122.0 | 121.8 | 121.6[c] | 121.3[d] |
| A(19,36,33) | 123.2 | 148.2 | 139.3 | 148.0 | 150.1[c] | 147.0[d] |

[a] Ref. [28].
[b] Ref. [29].
[c] Ref. [30].
[d] Ref. [31].

highest polarity L3 form has not appeared. The $CH_3OH$ solvent is a protic and polar solvent; this property makes it possible for both forms L3 and L4 to be stable in this solvent. The polarity of the solvent and hydrogen bond formation between solvent and title compound plays a main role in the formation and fixation of L3 form.

For this compound, the calculated harmonic oscillator model of aromaticity (HOMA) [27] index for the $C_{24}/C_{25}$ ring is 0.942 (see Figure 2). As expected, the aromaticity level of the $C_{24}/C_{25}$ ring decreases as the L4 form changed to the L3 form, and confirms that L4 form is more stable than L3 form.

Schiff bases show tautomerism by intramolecular proton transfer from oxygen atom to the nitrogen atom. As a result of this, Schiff bases can exist in two tautomeric structures as enol (O–H…N in enol-imine) and keto (N–H…O in keto-amine) form in the solid state. In order investigate the effects of proton transfer on molecular geometry a potential energy surface (PES) scan process done at the B3LYP/6-311++G(d,p) level (see Figure 3). In Figure 3a, the keto form is more stable than the enol form, 7.72 kcal/mol is needed for this conversion, and Figure 3b shows that the enol form is more stable and less energy (4.91 kcal/mol) is a required for exchange.

The optimized geometry of BrSEIPO is given in Figure 4, and geometrical parameters are listed in Table 2. To the best of our knowledge, exact experimental data on the geometrical parameters of BrSEIPO is not available in the literature. Therefore, the optimized structure can only be compared with other similar systems for which the crystal structures have been solved [28-31].

This table shows that the bond lengths and bond angles calculated in L3 and L4 forms are more consistent with the reported experimental results.

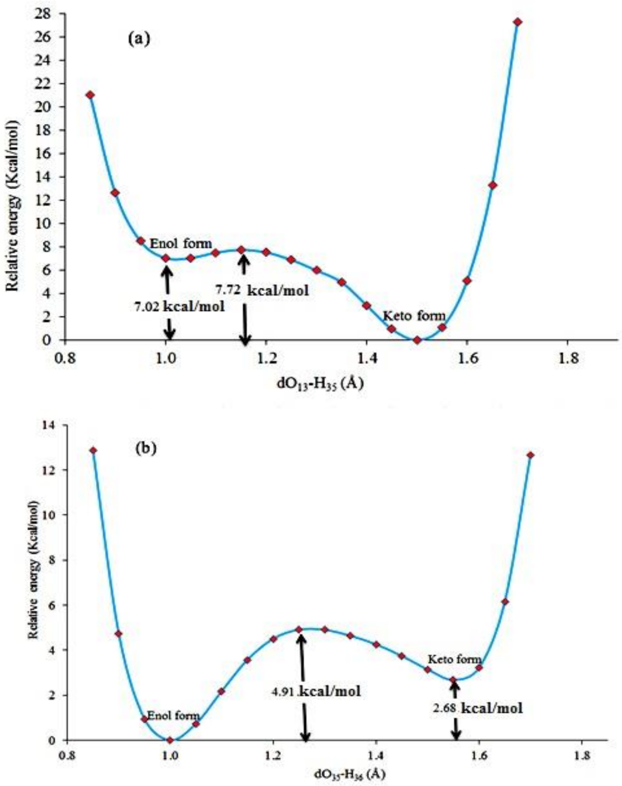


**Figure 3** Schematic energy profile of intramolecular proton transfer in gas phase; a) L1 form; b) L4 form.

The bond lengths of $C_2{=}O_{13}$=1.248 Å in L4, L3 forms, and $C_{22}{=}N_{19}$=1.283 Å in L4 form show that these bonds are of the double bond. Also, the bond length $C_{19}$–$N_{18}$ and $C_{14}$–$N_{15}$ are shorter than the normal C–N single bond length of about 1.48 Å.

**Table 3:** Calculated and observed $^1$H chemical shifts for the most stable tautomeric forms of BrSEIPO.

| | Theoretical | | |
|---|---|---|---|
| Assignment | L3 form | L4 form | Averaged values |
| $H_{10,11,12}$ | 1.881 | 1.784 | 1.832 |
| $H_{6,7,8}$ | 1.894 | 1.902 | 1.898 |
| $H_{21}$ | 3.327 | 3.235 | 3.281 |
| $H_{17}$ | 3.464 | 3.455 | 3.460 |
| $H_{16}$ | 3.864 | 3.669 | 3.767 |
| $H_{20}$ | 4.283 | 3.851 | 4.067 |
| $H_4$ | 5.082 | 5.170 | 5.126 |
| $H_{31}$ | 7.065 | 6.477 | 6.771 |
| $H_{32}$ | 7.336 | 7.054 | 7.195 |
| $H_{28}$ | 7.396 | 7.091 | 7.243 |
| $H_{23}$ | 8.514 | 7.752 | 8.133 |
| $H_{34}$ | 11.238 | 11.500 | 11.369 |
| $H_{36}$ | 13.191 | --- | --- |
| | --- | 14.073 | --- |

The bond angles $C_1$–$C_3$–$N_{14}$, $C_{24}$–$C_{22}$–$N_{19}$, $C_3$–$N_{15}$–$C_{16}$ and $C_{22}$–$N_{19}$–$C_{18}$ are about 120º which are consistent with the $sp^2$ hybrid character of $C_3$, $C_{23}$, $N_{14}$ and $N_{19}$ atoms [32]. In the keto-amine and enol-imine tautomers, the C–O and the C–N bonds are the double and single bonds, respectively.

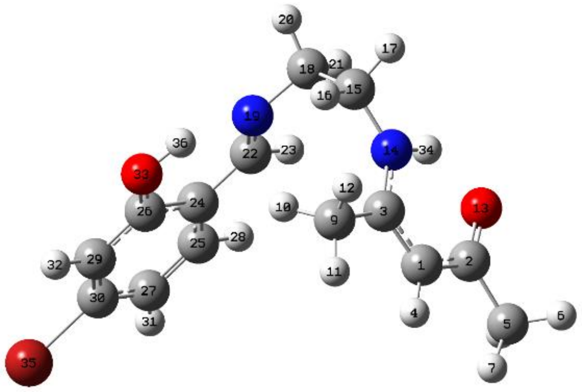


**Figure 4.** The theoretical geometric structure of the title compound (B3LYP/6-311++G(d,p) level), with the atom numbering.

### 3.2 NMR spectral studies

The $^1$H theoretical chemical shifts using the Gauge-Included Atomic Orbital (GIAO) method [33] and the assignments of BrSEIPO are presented in Table 3. In $^1$H NMR spectrum, the absorption peaks of the aromatic ring, methyl, ethane and imino proton the aliphatic protons are observed in 6.77–7.24, 1.83–1.89, 3.28–4.07 and 8.13 ppm. A singlet peak at 11.37 ppm is related to intramolecular hydrogen bonding ($O_{13}\cdot\cdot\cdot H_{34}$–$N_{14}$). The signals at $\delta$= 13.91 and $\delta$ = 14.07 are assigned to the keto-amine (NH) and enol-imine (OH) protons, respectively.

### 3.3 Intramolecular hydrogen bonding

Some spectroscopic properties, AIM results and the averaged values of some optimized geometrical parameters of the chelated rings, related to the hydrogen bond strength for BrSEIPO, SEIPO and APO [34] are listed in Table 4. According to Table 4, in BrSEIPO the averaged values of O…N and O…H distances decrease, while the OHN bond angle and N-H bond length increase in comparison with SEIPO and APO. This is due to of high steric effect o111f ethyl group. This is in agreement with the averaged of the AIM results (see Table 4). Rozas et al. [35] reported that medium hydrogen bonds show the Laplacian of electron density at the critical point ($\nabla^2\rho_{BCP}$) > 0 and the energy density at the bond critical point ($H_{BCP}$) < 0. The electron density at bond critical point ($\rho_{BCP}$) in BrSEIPO is greater than that of in SEIPO and APO. Thus, it is another evidence for the stronger IHB in BrSEIPO than that in SEIPO and APO. The hydrogen bond energy can be calculated using the relationship $E_{HB}=V(r_{BCP})/2$ described by Espinosa et al [36]. The average values of the $E_{HB}$ for BrSEIPO (11.03), SEIPO (10.97), and for APO (8.20), calculated at the B3LYP/6-311++G(d,p) level, are also compared in Table 4, which is in agreement with the above trend for IHB strength.

This result is consistent with the NMR proton chemical shift of 9.7 and 10.91 ppm for the hydrogen-bonded proton in APO [37] and SEIPO, respectively.

To increase the power of hydrogen bonding, its better the proton chemical shift (δOH) and out-of-plane bending mode frequency (γNH) increase, and also the stretching mode frequency (νNH) decrease. By comparing the value of these quantities that presented in Table 4, the following trend in hydrogen bond strength is concluded: BrSEIPO > SEIPO > APO

To increase the power of hydrogen bonding, its better the OHO bond angle, N-H bond length, electron density at bond critical point ($\rho_{BCP}$), hydrogen bond energy ($E_{HB=}$ $V(r_{BCP})/2$ [36]), proton chemical shift (δOH) and out-of-plane bending mode frequency (γNH) increase, and also the O…N, O…H distances and stretching mode frequency (νNH) decrease. By comparing the value of these quantities that presented in Table 4, the following trend in hydrogen bond strength is concluded: BrSEIPO > SEIPO > APO

### 3.4 NBO analysis

To understand the charge redistribution in the BrSEIPO, the NBO analysis for calculating the natural atomic charges and charge transfer energies ($E^2$) over all atoms involved in the chelated ring specially between the lp(O) →σ*N–H and lp(N) →σ*O–H in gas phase and different solvents in order to understand the solvent effects on interactions done by using NBO 3.1 program [38] and listed in table 5. By increasing of hydrogen bond strength, electron resonance in the chelate ring increases. With increasing the polarity of solvents the charge transfer energies ($E^2$) for LP($O_{13}$)→ BD*$N_{14}$-$H_{34}$ reduced whereas LP($O_{33}$)→ BD*$N_{19}$-$H_{36}$ and LP($N_{19}$)→ BD*$O_{33}$-$H_{36}$ interactions increases and decrease, respectively. Actually, L3 form becomes more stable with increasing solvent polarity.

5. In Figure 5, this molecule has several possible sites for the electrophilic attacks over the nitrogen and oxygen atoms with the fitting point charge -0.675 ($O_{13}$), -0.604 ($N_{14}$) -0.682 ($O_{33}$), -0.537 ($N_{19}$) (The values are for the more stable L4). Also, maximum positive and negative potential regions are localized to the hydrogen atoms (particular H atoms of ethane) and electronegative atoms indicating possible sites for nucleophilic and electrophilic attacks.

**Table 4:** Comparing several properties related to the hydrogen bond strength ($O_{13}H_{34}N_{14}$) for BrSEIPO, SEIPO, and APO (All calculated at the B3LYP/6-311++G(d,p) level).

| | BrSEIPO | SEIPO[d] | APO[e] |
|---|---|---|---|
| *Geometrical results*[a] | | | |
| RO…N | 2.650 | 2.652 | 2.666 |
| RN–H | 1.029 | 1.028 | 1.019 |
| O…H | 1.792 | 1.794 | 1.885 |
| θOHN | 138.6 | 138.5 | 130.9 |
| *AIM results*[b] | | | |
| $\rho_{BCP}$ | 0.0401 | 0.0399 | 0.0324 |
| $\nabla^2\rho_{BCP}$ | 0.0331 | 0.0330 | 0.0290 |
| $H_{BCP}$ | -0.0352 | -0.0350 | -0.0014 |
| H-bond energy | 11.0296 | 10.9679 | 8.2048 |
| *Spectroscopic result*[c] | | | |
| νNH | 3148 | 3151(3060) | 3422(3179) |
| γNH | 849 | 847(836) | 811(818) |
| δOH | 11.37 | 11.36(10.91) | 10.26(9.7[f]) |

[a] R is the intramolecular O…N, N–H, O…H distances in Å, θ: the hydrogen bond angle N-H…O in degree (for BrSEIPO, the average values are given).
[b] The units of AIM results are: $\rho_{BCP}$ (e au$^{-3}$), $\nabla^2\rho_{BCP}$ (e au$^{-5}$), $H_{BCP}$ (hartree au$^{-3}$) and H-bond energy (kcal/mol).
[c] ν and γ are stretching and out-of-plane bending modes frequencies, respectively, in cm$^{-1}$. δ, proton chemical shift in ppm. (Experimental values are given in parenthesis).
[d] Data source: Ref. [22].
[e] Data source: Ref. [34].
[f] Data source: Ref. [37].

**Table 5:** Second order perturbation theory analysis of the fock matrix in NBO basis in different solvents.

| | L4 form | | | L3 form | | |
|---|---|---|---|---|---|---|
| Solvent | Donor | Acceptor | $E^2$ | Donor | Acceptor | $E^2$ |
| Gas phase | LP(2)$O_{13}$ | BD*(1)$N_{14}$-$H_{34}$ | 13.18 | LP(2)$O_{13}$ | BD*(1)$N_{14}$-$H_{34}$ | 13.91 |
| | LP(1)$N_{19}$ | BD*(1)$O_{33}$-$H_{36}$ | 20.37 | LP(1)$O_{33}$ | BD*(1)$N_{19}$-$H_{36}$ | 25.71 |
| $CCl_4$ | LP(2)$O_{13}$ | BD*(1)$N_{14}$-$H_{34}$ | 11.95 | LP(2)$O_{13}$ | BD*(1)$N_{14}$-$H_{34}$ | 12.63 |
| | LP(1)$N_{19}$ | BD*(1)$O_{33}$-$H_{36}$ | 17.47 | LP(1)$O_{33}$ | BD*(1)$N_{19}$-$H_{36}$ | 27.30 |
| $CH_2Cl_2$ | LP(2)$O_{13}$ | BD*(1)$N_{14}$-$H_{34}$ | 10.49 | LP(2)$O_{13}$ | BD*(1)$N_{14}$-$H_{34}$ | 10.88 |
| | LP(1)$N_{19}$ | BD*(1)$O_{33}$-$H_{36}$ | 13.86 | LP(1)$O_{33}$ | BD*(1)$N_{19}$-$H_{36}$ | 29.55 |
| EtOH | LP(2)$O_{13}$ | BD*(1)$N_{14}$-$H_{34}$ | 10.53 | LP(2)$O_{13}$ | BD*(1)$N_{14}$-$H_{34}$ | 10.83 |
| | LP(1)$N_{19}$ | BD*(1)$O_{33}$-$H_{36}$ | 13.75 | LP(1)$O_{33}$ | BD*(1)$N_{19}$-$H_{36}$ | 29.48 |
| $CH_3CN$ | LP(2)$O_{13}$ | BD*(1)$N_{14}$-$H_{34}$ | 10.47 | LP(2)$O_{13}$ | BD*(1)$N_{14}$-$H_{34}$ | 10.81 |
| | LP(1)$N_{19}$ | BD*(1)$O_{33}$-$H_{36}$ | 13.72 | LP(1)$O_{33}$ | BD*(1)$N_{19}$-$H_{36}$ | 29.57 |

[a] $E^2$ means energy of hyper-conjugative interactions (stabilization energy in kcal/mol)

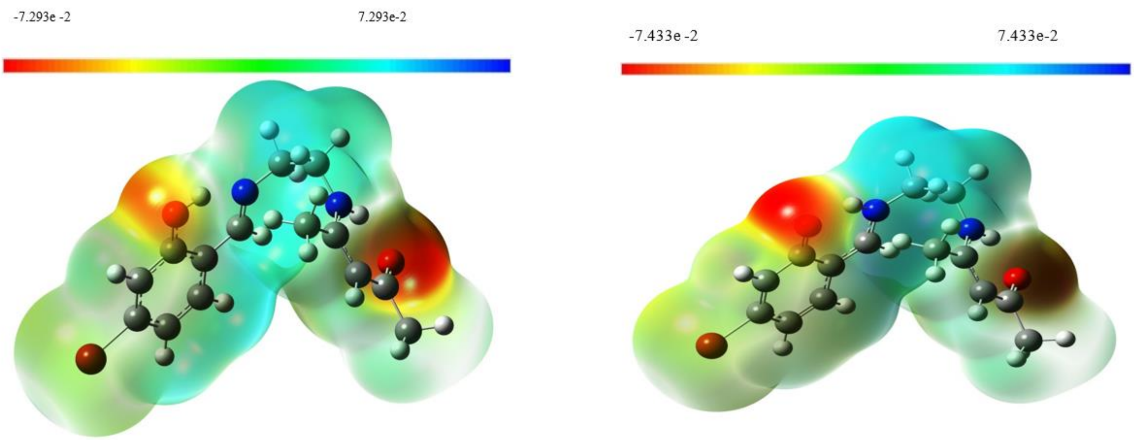


**Figure 5.** Molecular electrostatic potential surface for L3 and l4 forms calculated by B3LYP/6-311G++(d,p) level. (For interpretation of the references to color in this figure, the reader is referred to the web version of the article.)

### ***3.5 Molecular electrostatic potential (MEP) surface***

The plot of the MEP (3D) reveals maximum values of positive and negative potentials corresponding to chemical reactivity (electrophilic and nucleophilic region). The 3D plot of the MEP surface for the DABMISO is shown in Figure

From figure 5 it can be concluded that the strong and weak negative area associated with the O and N atoms and the feeble positive area of the around $H_{14}$, $H_{36}$ atoms are the demonstrator of intramolecular (intramolecular ($O_{13}…H_{34}–N_{14}$, $N_{19}…H_{36}–O_{33}$) hydrogen bonding.

**Table 6** Calculated absorption wavelengths and oscillator strengths of L3 and L4 forms.

| Solvent | Calculated (L3 form) | | | Calculated (L4 form) | | |
|---|---|---|---|---|---|---|
| | λ(nm) | *f* | Major contribution (≥10%) | λ(nm) | *f* | Major contribution (≥10%) |
| $CCl_4$ | 383 | 0.1408 | H→ L(75%), H-1→ L(24%) | | | |
| | 367 | 0.0804 | H-1→ L(75%), H→ L(23%) | 352 | 0.0322 | H→ L(100%) |
| | 304 | 0.0002 | H-2→ L(69%), H-2→ L+1(30%) | 302 | 0.2338 | H-1→ L(88%) |
| | 294 | 0.0233 | H→ L+1(74%), H-2→ L+1(15%) | 279 | 0.3429 | H→ L+1(86%), H-3→ L(10%) |
| | | | | 266 | 0.0018 | H-4→ L(96%) |
| $C_2H_5OH$ | 382 | 0.1337 | H→ L(75%), H-1→ L(24%) | | | |
| | 366 | 0.0796 | H-1→ L(75%), H→ L(23%) | 348 | 0.0282 | H→ L(100%) |
| | 303 | 0.0003 | H-2→ L(66%), H-2→ L+1(33%) | 301 | 0.2241 | H-1→ L(88%) |
| | 293 | 0.0269 | H→ L+1(94%) | 279 | 0.0150 | H-2→ L(90%) |
| | | | | 266 | 0.0035 | H-4→ L(95%) |

For both L3 and L4 forms in $CCl_4$ and $C_2H_5OH$ solvents, wavelength (λ), oscillator strength (*f*) and major contributions of transitions calculated and compared with experimental results (see Table 6).

## 4. Conclusion

The tautomeric equilibria in 5-Bromo-salicylideneiminpo-ethylimino-pentan-2-one and tautomerism in selected solvents have been studied. The results showed that the L4 and L3 forms are the more stable forms with 99.29% and 0.71% values in the gas phase. The L3 form has more polarity than L4 form; therefore, with increasing solvent polarity L3 form becomes more stable and the molar fraction increases from 0.87 to 32.09. By comparing the value of the effective parameters for the hydrogen bond (AIM results, spectroscopic properties and optimized geometrical parameters), the following trend in hydrogen bond strength is concluded: BrSEIPO > SEIPO > APO.

**Acknowledgments**:

The authors are thankful to Ferdowsi University of Mashhad for the partial support of the work.

## References:

[1] Liu, J.; Zhang, B.; Wu, B.; Zhang, K.; Hu, S. The direct electrochemical synthesis of Ti (II), Fe (II), Cd (II), Sn (II), and Pb (II) complexes with N, N-bis (Salicylidene)-o-phenylenediamine. *Turkish Journal of Chemistry* **2007**, *31* (6), 623-629.

[2] Le Bozec, H.; Renouard, T. Dipolar and Non-Dipolar Pyridine and Bipyridine Metal Complexes for Nonlinear Optics. *European Journal of Inorganic Chemistry* **2000**, *2000* (2), 229-239.

[3] Ünver, H.; Karakas, A.; Elmali, A. Nonlinear optical properties, spectroscopic studies and structure of 2-hydroxy-3-methoxy-N-(2-chloro-benzyl)-benzaldehyde-imine. *Journal of molecular structure* **2004**, *702* (1), 49-54.

(4) Cummings, S. D.; Cheng, L.-T.; Eisenberg, R. Metalloorganic Compounds for Nonlinear Optics: Molecular Hyperpolarizabilities of M (diimine)(dithiolate) Complexes (M= Pt, Pd, Ni). *Chemistry of materials* **1997**, *9* (2), 440-450.

(5) Lenoble, G.; Lacroix, P. G.; Daran, J. C.; Di Bella, S.; Nakatani, K. Syntheses, crystal structures, and NLO properties of new chiral inorganic chromophores for second-harmonic generation. *Inorganic chemistry* **1998**, *37* (9), 2158-2165.

[6] Lacroix, P. G.; Di Bella, S.; Ledoux, I. Synthesis and second-order nonlinear optical properties of new copper (II), nickel (II), and zinc (II) Schiff-base complexes. Toward a role of inorganic chromophores for second harmonic generation. *Chemistry of materials* **1996**, *8* (2), 541-545.

[7] Coe, B. J.; Houbrechts, S.; Asselberghs, I.; Persoons, A. Efficient, Reversible Redox-Switching of Molecular First Hyperpolarizabilities in Ruthenium (II) Complexes Possessing Large Quadratic Optical Nonlinearities. *Angewandte Chemie International Edition* **1999**, *38* (3), 366-369.

[8] Coe, B.; Harris, J.; Jeffery, J.; Rees, L.; Hursthouse, M. Tuning of charge-transfer absorption and molecular quadratic non-linear optical properties in ruthenium (II) ammine complexes†. *Journal of the Chemical Society, Dalton Transactions* **1999**, (20), 3617-3625.

[9] Atkins, R.; Brewer, G.; Kokot, E.; Mockler, G. M.; Sinn, E. Copper (II) and nickel (II) complexes of unsymmetrical tetradentate Schiff base ligands. *Inorganic Chemistry* **1985**, *24* (2), 127-134.

[10) Gradinaru, J.; Forni, A.; Druta, V.; Tessore, F.; Zecchin, S.; Quici, S.; Garbalau, N. Structural, spectral, electric-field-induced second harmonic, and theoretical study of Ni (II), Cu (II), Zn (II), and VO (II) complexes with [N2O2] unsymmetrical Schiff bases of S-methylisothiosemicarbazide derivatives. *Inorganic chemistry* **2007**, *46* (3), 884-895.

[11) Türkoğlu, G.; Berber, H.; Dal, H.; Öğretir, C. Synthesis, characterization, tautomerism and theoretical study of some new Schiff base derivatives. *Spectrochimica Acta Part A: Molecular and Biomolecular Spectroscopy* **2011**, *79* (5), 1573-1583.

[12) Eshghi, H.; Seyedi, S. M.; Safaei, E.; Vakili, M.; Farhadipour, A.; Bayat-Mokhtari, M. Silica supported Fe (HSO 4) 3 as an efficient, heterogeneous and recyclable catalyst for synthesis of β-enaminones and β-enamino esters. *Journal of Molecular Catalysis A: Chemical* **2012**, *363*, 430-436.

[13) Weinstein, J.; Wyman, G. A Study of β-Amino-α, β-unsaturated Ketones1. *The Journal of Organic Chemistry* **1958**, *23* (11), 1618-1622.

[14] Tayyari, S. F.; Raissi, H.; Tayyari, F. Vibrational assignment of 4-amino-3-penten-2-one. *Spectrochimica Acta Part A: Molecular and Biomolecular Spectroscopy* **2002**, *58* (8), 1681-1695.

[15] Jeffrey, G. A.; Saenger, W. *Hydrogen bonding in biological structures*; Springer Science & Business Media, 2012.

[16] Desiraju, G. R.; Steiner, T. *The weak hydrogen bond: in structural chemistry and biology*; Oxford University Press on Demand, 2001.

[17] Desiraju, G. R. Supramolecular synthons in crystal engineering—a new organic synthesis. *Angewandte Chemie International Edition in English* **1995**, *34* (21), 2311-2327.

[18] Fahid, F.; Kanaani, A.; Pourmousavi, S. A.; Ajloo, D. Synthesis, tautomeric stability, spectroscopy and computational study of a potential molecular switch of (Z)-4-(phenylamino) pent-3-en-2-one. *Molecular Physics* **2017**, *115* (7), 795-808.

[19] Kanaani, A.; Ajloo, D.; Kiyani, H.; Ghasemian, H.; Vakili, M.; Feizabadi, M. Molecular structure, spectroscopic investigations and computational study on the potential molecular switch of (E)-1-(4-(2-hydroxybenzylideneamino) phenyl) ethanone. *Molecular Physics* **2016**, *114* (13), 2081-2097.

[20] Dudek, G.; Dudek, E. P. Spectroscopic studies of keto–enol equilibria. Part XIII. 15 N-substituted imines. *Journal of the Chemical Society B: Physical Organic* **1971**, 1356-1360.

[21] Bertolasi, V.; Pretto, L.; Ferretti, V.; Gilli, P.; Gilli, G. Interplay between steric and electronic factors in determining the strength of intramolecular N—H··· O resonance-assisted hydrogen bonds in β-enaminones. *Acta Crystallographica Section B: Structural Science* **2006**, *62* (6), 1112-1120.

[22] Kanaani, A.; Ajloo, D.; Grivani, G.; Ghavami, A.; Vakili, M. Tautomeric stability, molecular structure, NBO, electronic and NMR analyses of salicylideneimino-ethylimino-pentan-2-one. *Journal of Molecular Structure* **2016**, *1112*, 87-96.

[23] Frisch, M.; Trucks, G.; Schlegel, H.; Scuseria, G.; Robb, M.; Cheeseman, J.; Montgomery Jr, J.; Vreven, T.; Kudin, K.; Burant, J. Gaussian 03, revision c. 02; Gaussian. *Inc., Wallingford, CT* **2004**, *4*.

[24] Mennucci, B.; Tomasi, J. Continuum solvation models: A new approach to the problem of solute's charge distribution and cavity boundaries. *The Journal of chemical physics* **1997**, *106* (12), 5151-5158.

[25] Biegler Konig, F.; Schonbohm, J.; Bayles, D. Software news and updates AIM2000. *J Comput Chem* **2001**, *22*, 545-559.

[26] Hür, D.; Güven, A. The acidities of some indoles. *Journal of Molecular Structure: THEOCHEM* **2002**, *583* (1), 1-18.

[27] Krygowski, T. M.; Cyranski, M. K. Structural aspects of aromaticity. *Chemical reviews* **2001**, *101* (5), 1385-1420.

[28] Özkar, S.; Ülkü, D.; Yıldırım, L. T.; Biricik, N.; Gümgüm, B. Crystal and molecular structure of bis (acetylacetone) ethylenediimine: intramolecular ionic hydrogen bonding in solid state. *Journal of molecular structure* **2004**, *688* (1-3), 207-211.

(29] Benjelloun, O.; Akkurt, M.; Yıldırım, S.; Daoudi, M.; Larbi, N. B.; Kerbal, A.; Bennani, B.; Büyükgüngör, O.; Jalbout, A.; Haddae, T. B. B3LYP theoretical calculations and structure of 4-[(2-{[(1E)-1-methyl-3-oxobutylidene] amino} ethyl) imino] pentan-2-one. *ARKIVOC* **2008**, *11*, 56-63.

[30] Dziembowska, T.; Ambroziak, K.; Majerz, I. Analysis of the vibrational spectra of trans-N, N'-bis-salicylidene-1', 2'-cyclohexanediamine tautomers. *Journal of molecular structure* **2005**, *738* (1-3), 15-24.

[31] Mota, V. Z.; de Carvalho, G. S.; Corbi, P. P.; Bergamini, F. R.; Formiga, A. L.; Diniz, R.; Freitas, M. C.; da Silva, A. D.; Cuin, A. Crystal structure and theoretical studies of the keto-enol isomerism of N, N'-bis (salicylidene)-o-phenylenediamine (salophen). *Spectrochimica Acta Part A: Molecular and Biomolecular Spectroscopy* **2012**, *99*, 110-115.

[32] Khalaji, A. D.; Grivani, G.; Seyyedi, M.; Fejfarova, K.; Dusek, M. Zinc (II) and mercury (II) complexes [Zn ((2, 6-Cl-ba) 2 en) I 2] and [Hg ((2, 6-Cl-ba) 2 en) Br 2] with the bidentate Schiff base ligand (2, 6-Cl-ba) 2 en: Synthesis, characterization and crystal structures. *Polyhedron* **2013**, *49* (1), 19-23.

[33] Frisch, M. J.; Pople, J. A.; Binkley, J. S. Self-consistent molecular orbital methods 25. Supplementary functions for Gaussian basis sets. *The Journal of chemical physics* **1984**, *80* (7), 3265-3269.

[34] Berenji, A. R.; Tayyari, S. F.; Rahimizadeh, M.; Eshghi, H.; Vakili, M.; Shiri, A. *Book of Abstracts of 15th Iranian Chemistry Congress*; 2001.

[35] Rozas, I.; Alkorta, I.; Elguero, J. Behavior of ylides containing N, O, and C atoms as hydrogen bond acceptors. *Journal of the American Chemical Society* **2000**, *122* (45), 11154-11161.

[36] Espinosa, E.; Molins, E.; Lecomte, C. Hydrogen bond strengths revealed by topological analyses of experimentally observed electron densities. *Chem. Phys. Lett.* **1998**, *285* (3), 170-173.

[37] SDBSWeb, National Institute of Advanced Industrial Science and Technology, 2012.http://riodb01.ibase.aist.go.jp/sdbs/.

[38] Glendening, E.; Reed, A.; Carpenter, J.; Weinhold, F. NBO Version 3.1, TCI. *University of Wisconsin, Madison* **1998**, *65*.